Perceptual validation of wind turbine noise auralization

Julien Maillard, Andrea P C Bresciani, Arthur Finez

forum acusticum 2023

PERCEPTUAL VALIDATION OF WIND TURBINE NOISE AURALIZATION

Julien Maillard[1] **Andrea P. C. Bresciani**[1] **Arthur Finez**[2]

[1] Centre Scientifique et Technique du Bâtiment (CSTB), Saint-Martin-d'Hères, 38400, France
[2] ENGIE Green, Lyon, France

ABSTRACT

Wind turbine noise is often mentioned as one of the limitations restraining the deployment of wind energy in rural areas. So far, the mechanisms behind the noise annoyance induced by wind turbines have been studied mostly using field recordings. However, optimizing the design, location and operation of modern wind turbines to both increase energy production and limit noise pollution clearly benefits from accurate prediction models. Work in this field has received much interest and physics-based models of wind turbine noise have been developed. Recently, such a model has been proposed by the authors where equivalent sources representing the leading- and trailing-edge noise emission of the blades are characterized using Amiet's theory and RANS simulations. These sources are then propagated in the far-field using standardized engineering models suited to take into account topography, ground properties, atmospheric and weather effects. Furthermore, an auralization technique allows the generation of audio signals for 3D noise rendering and perceptual evaluation. In this paper, the performance of the proposed auralization system is evaluated through listening tests comparing recorded and auralized wind turbine noise. Recorded samples were obtained on an existing site, with dedicated instrumentation to measure the environmental noise under different wind conditions at several locations.

Keywords: *wind turbine noise, auralization, acoustic emission and propagation modeling*

Corresponding author: julien.maillard@cstb.fr.

1. INTRODUCTION

The need for renewable energy has pushed for a significant increase in wind turbine installations. For on-shore installation, the acoustic impact of wind turbines on nearby dwellings is subject to specific regulations, based on e.g., distance to the dwelling and emergence above background noise. These regulations are justified by the noise annoyance caused by wind turbines under certain conditions. For instance, Janssen *et al.* [1] found that wind turbine noise is declared as the most annoying sound source compared to other sources such as wind, road, and rail, despite having lower or similar sound levels. Therefore, wind turbine manufacturers and operators seek to increase energy production on one hand, while reducing noise annoyance and complying with regulations on the other hand. This requires optimizing the design, location, and operation of the wind turbines.

Regarding noise emission, the optimization process would greatly benefit from simulation tools capable of accurately predicting noise levels radiated by wind turbines under specific conditions. For this reason, much research has been carried out in recent years to develop and improve such simulation tools. Furthermore, the need to auralize wind turbine noise has also emerged to help study and understand the mechanisms of noise annoyance. In this case, auralization allows to assess wind turbine noise annoyance for various conditions through listening tests. Such tools may prove also valuable to promote acceptance of wind turbines by demonstrating their acoustic impact through augmented reality applications based on accurate auralized soundscapes.

Previous work on auralization of wind turbine noise includes signal-based auralization and physics-based auralization. Pieren [2] proposed a sample-based methodology where recorded samples are used to obtain the parameters of the synthesized signal, which includes a tonal component and an amplitude-modulated broadband part. Results from listening tests comparing real audio recordings with synthetic signals indicated an acceptable level of realism. This type of approach is however limited by the restricted number of modeled scenarios imposed by the conditions of the recording. On the other hand, physics-based auralization uses a numerical model whose parameters may be freely adjusted to address a wider range of configurations. This is the approach adopted in the present work. It requires modeling first the aerodynamic noise emission of the wind turbine, which is the dominant noise source, and second, its propagation to the receiver. The frequency and time-dependent characteristics of the noise emission and atmospheric propagation models are then applied to appropriate signal processing algorithms in order to construct a spatialized 3D audio signal at the receiver location.

A cost-efficient modeling approach for the source emission is based on Amiet's theory [3, 4]. This model can then be coupled with ray-tracing or parabolic equation methods to obtain the noise levels in the far field, taking into account ground and atmospheric propagation effects. Recently, Mascarenhas [5] developed a physics-based approach for the auralization of wind turbine noise. The approach is based on the decomposition of each turbine blade into elementary short segment sources, whose acoustic radiation in the far field is obtained by coupling Amiet's emission model with the parabolic equation [6]. Short-time signals associated with different blade segments at different angular positions are then calculated based on the radiated sound pressure level at the receiver location. These short time signals are finally cross-faded using an appropriate window function to construct the signal for a complete blade rotation.

Unlike the method above, the approach used in the present work employs a continuous time signal, obtained by noise shaping synthesis, which is amplitude modulated and delayed based on the time-dependent noise levels computed for discrete blade segment positions. As a result, the method allows for a continuous time-varying delay, thus properly rendering Doppler shifts. Another advantage of the method is to decouple the calculation of the emission source signals from the far-field propagation effect rendering. This facilitates integrating the method in previously developed auralization systems [7–9] to combine wind turbine sources with other noise sources such as road or railway traffic noise. Similar to previous work, e.g. [10, 11], the wind turbine blade is decomposed in a set of short blade segments where the acoustic radiation of each segment is modeled by a single aerodynamic elementary source. This source power and directivity is computed using a RANS-based Amiet's theory for leading- and trailing-edge noise [3, 4]. The contribution of each elementary source to the receiver located in the far field is then calculated using engineering ray-based methods for outdoor sound propagation. Compared to the parabolic equation or standard ray tracing in refracting medium, these engineering models have a much lower computational cost while still providing sufficient accuracy at distances commonly encountered for wind turbine sound propagation. The approach can therefore be applied to wind farms with multiple wind turbines in complex environments including topography, buildings, as well as other noise sources. In this work, the Harmonoise model [12, 13] is implemented as it includes a more refined meteorological model taking into account refraction due to specific wind conditions as well as turbulence scattering effects.

The overall process includes two distinct steps. First, the blade segment emission characteristics is computed for potentially multiple blade geometries and operating conditions such as wind and rotational speed. Second, the transfer functions between elementary blade source positions and receivers are obtained, followed by the averaged sound pressure levels over one blade rotation and the auralized audio samples using the emission database from the first step. This second phase has been integrated into CSTB's outdoor noise auralization software, MithraSOUND®. For a more detailed description of the complete workflow and underlying theory, the reader is referred to recently published work by the authors [14–17].

The present paper describes the first results of the validation of the approach against on-site measurements of operating wind turbines. The validation consists in first comparing the measured sound pressure levels at different locations around the wind turbines with those obtained at the same locations with the proposed approach. Second, the realism of the auralized signals is evaluated through listening tests mixing recorded audio signals of the real environments and auralized signals of the simulated environment.

The measurement site and recorded audio samples are presented in Section 2, followed in Section 3 by the modeling

of the site and the generation of auralized audio samples. Results are discussed in Section 4.

Figure 1: View of one of the measurement point upwind of the wind turbine. The microphone is placed on a hard 1 m diameter board and protected by a windscreen according to IEC 61400 specifications.

2. MEASUREMENT SITE

The measured data was collected on an existing site, equipped with five 2 MW wind turbines of rotor diameter, 92 m, and hub height, 100 m. The terrain can be considered flat with cultivated fields of the same type. Acoustic measurements used Class 1 sound level meters positioned at various locations, upwind, downwind, and in the crosswind directions of the wind turbines, with distances from 150 m, i.e., close to the machines, according to the IEC 61400 standard specifications, up to 1.5 km. Measured data includes continuous 1/3 octave band equivalent levels between 12.5 Hz and 20 kHz with a 1 s integration constant. In parallel, the measured sound pressure signal was recorded at a 25.6 kHz sampling frequency for listening tests and additional frequency analysis. Simultaneous meteorological data was measured using a LiDAR system, six 3D sonic anemometers and a 100 m mast equipped with several anemometers and thermometers. The standard deviation of the velocity measured by the LiDAR system, at 100 m, is used for the numerical simulations. The humidity is also measured and used in the simulations. Finally, wind turbine operation data were also collected including rotational speed, blade pitch angle, and wind speed and wind direction at hub height. Fig. 1 shows a view of one of the IEC 61400 measurement point upwind of the wind turbine.

The results presented in this paper include two sets of wind turbine Operating Conditions (OC), referred to as OC1 and OC2, whose parameters are taken from two different time periods during the measurement campaign, and three receiver locations, referred to as SB1, SB2, and SB3, corresponding to three IEC measurement points, i.e., at a 150 m distance, for the North wind turbine, as will be shown in Fig. 3. Condition OC1 corresponds to a 12.2 m/s wind speed at hub height, with orientation 220 deg measured counter-clockwise from the North, a 15.1 rpm rotor rotational speed, and a 7.8 deg blade pitch angle. Condition OC2 corresponds to a 7.54 m/s wind speed, with orientation 259 deg, rotor speed, 13.72 rpm, and a 0 deg blade pitch angle. Note that these two conditions are representative of the middle point and upper limit of the range of the most encountered operating conditions. During the measurements, the wind turbines were programmed to start and stop at prescribed times. By considering measured data before and after a stop time, the noise levels and associated audio recordings can be obtained for both total noise (i.e., including both turbine and background noise), and background noise, respectively. As an example, Fig. 2 presents the total and background noise levels for receiver SB1. As can be seen, the wind turbine noise is predominant at the short IEC distances for frequencies up to 4 kHz.

3. AURALIZED AUDIO SAMPLES

The numerical workflow starts from the 3D CAD of the wind turbine blade. As the CAD of the measured wind turbine was not available for this study, the blade of the generic SWT 2.3-93 (2.3 MW rated power and 93 m diameter) wind turbine [18, 19] is used instead. The two turbines belong to the same class and have similar rated power and diameter. The wind turbine blade is decomposed into 6 blade segments. The methodology is based on a RANS-informed Amiet's model [4] trailing-edge noise. The mid-span airfoil of each segment is used in

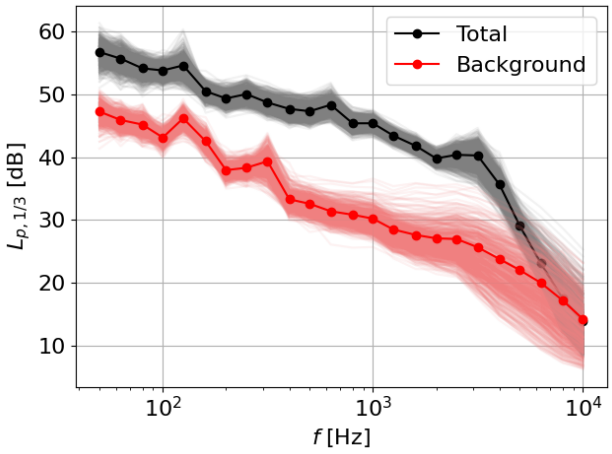

(a)

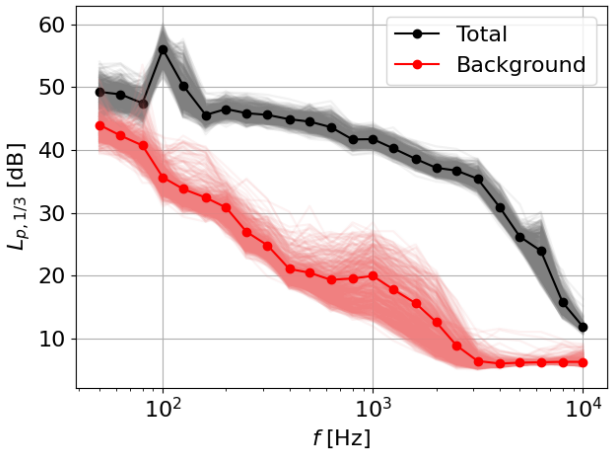

(b)

Figure 2: Total and background noise levels at receiver SB1, i.e., 150 m from the turbine, for operating conditions OC1 (a) and OC2 (b). The thin lines represent the 1 s equivalent levels and the thick lines, the overall average levels.

a 2D Reynolds-averaged Navier–Stokes (RANS) simulation to compute the boundary layer parameters required by Amiet's theory for trailing-edge noise. The leading-edge noise is also considered using Amiet's theory [3]. The von Karman turbulence spectrum is used to model the velocity spectrum with a turbulence intensity of 13.0% of the wind speed for OC1 and 7.75% for OC2. These values were measured by the LiDAR system at 100 m above the ground. The integral length scale was not measured. A reasonable value for flat terrain and neutral atmosphere is around 300 m and this value is used in the simulations. For each blade segment, the far-field radiated power and directivity data are computed for both operating conditions, OC1 and OC2. The details regarding the numerical workflow can be found in reference [17]. The measurement site is then modeled in MithraSOUND®, including the 5 wind turbines and a set of receiver points according to the measurement locations, as shown in Fig. 3. The three IEC receiver locations considered in this paper, SB1, SB2, and SB3, are approximately downwind, crosswind, and upwind, respectively, as can be seen from the wind direction of operating conditions OC1 and OC2 also shown in the figure.

The meteorological conditions for the numerical simulations were taken from the database of reference [20] for the closest airport. Both conditions correspond to night time with a nebulosity of approximately 2 okta for OC1 and 8 okta for OC2, a wind speed (10 m above ground) of 8.3 m/s for OC1 and 5.1 m/s for OC2. Temperature and humidity were, respectively, 5° C and 86% for OC1 and 8° C and 98% for OC2.

First, the averaged sound pressure levels are calculated

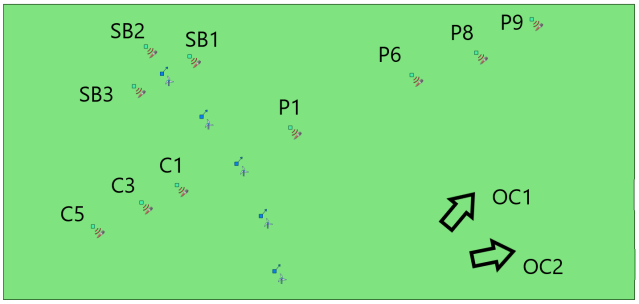

Figure 3: MithraSOUND® 2D view of the modeled site including the 5 wind turbines and the 3 receivers SB1, SB2 and SB3. Wind direction for both conditions OC1 and OC2 is shown at the bottom right.

over the wind turbine rotation period for the three receivers and the two operating conditions. The levels are obtained in each 1/3 octave band between 50 Hz and 10 kHz. They include the contributions from the 5 modeled wind turbines. For comparison with the measured total noise levels, the measured averaged background noise levels (see Fig. 2) are added to the calculated levels. Second, auralized signals are generated for the same receivers and operating conditions. Only the turbine closest to the receivers is included in the audio signals. The duration of the samples is 15 s, to match the duration of the recorded audio samples. The background noise is added to the synthetic wind turbine noise signals to allow comparison of recorded and auralized noise samples. The auralized signals are generated using mono rendering to match the omni-directional microphone recordings obtained from the measurements.

As an example, Fig. 4 shows the spectrogram of the auralized (top) and recorded (bottom) signals for receiver SB2 and operating conditions OC2. It can be seen that

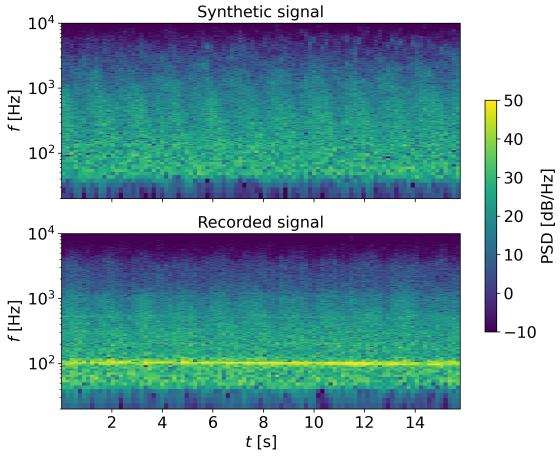

Figure 4: Spectrogram of auralized (top) and recorded (bottom) samples for receiver SB2 and operating conditons OC2. The spectrogram is obtained with a block size of 8192 samples and a Tukey window with 25% overlap.

the recorded and auralized spectrograms show similar features. In particular, the amplitude modulation associated with the blade motion is visible as expected from the position of receiver SB2 close to the crosswind direction. However, the recorded signal also presents a tonal noise around 100 Hz, not seen in the auralized signal. Listening to the audio samples suggests that this tone might be due to the mechanical noise of the turbine hub which can be heard in these conditions (OC2). It should also be mentioned that the auralized signals include the recently implemented amplitude fluctuations method [16] which was developed to increase the realism of auralized sources propagating through turbulent atmosphere. Even though, the propagation distance is relatively small for the studied receivers, this effect can still be seen in the spectrogram shown in Fig. 4.

4. VALIDATION RESULTS

This section presents first the comparison of the calculated and measured sound pressure levels. Results from listening tests based on a set of auralized and recorded audio samples are then discussed.

4.1 Level comparison

Fig. 5 shows the averaged 1/3 octave band spectra obtained for operating conditions OC1, for the three receivers SB1, SB2, and SB3, approximately in the upwind, crosswind and downwind direction, respectively (see Fig. 3). The numerical results well capture both the

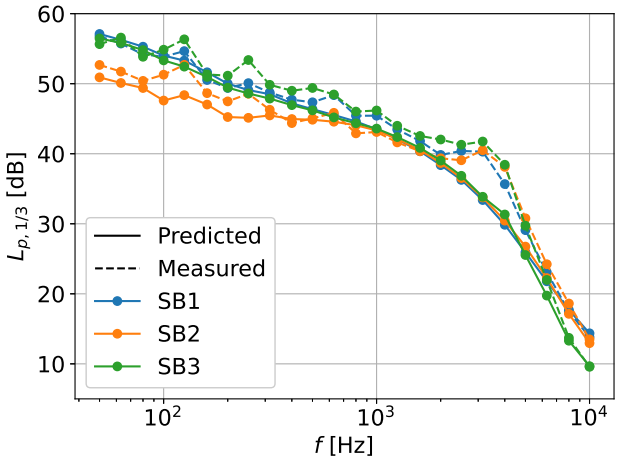

Figure 5: Comparison of the measured (dashed lines) and auralized (solid lines) 1/3 octave band levels for receivers SB1, SB2, and SB3, and operating conditions OC1.

spectrum shape and the absolute levels of the measure-

ments. Overall, the calculated levels slightly underestimate the measured levels by approximately 2 dB at most frequencies. The larger difference of up to 4 dB in the 125 Hz band, especially for receiver SB2, is due to an additional noise source, likely of mechanical origin. This noise source, not included in the model, yields a tone and some harmonics, which can be seen on a narrow band spectrum of the recorded audio signal (not shown here) and identified by careful listening. In the 3150 Hz band, the difference reaches approximately 8 dB. Listening to the recorded audio samples reveals that the associated amplitude increase might be due to blunt trailing-edge noise, which is not modeled in the auralization. Note that this type of noise, due to the finite size of the trailing edge, is usually absent in more recent wind turbine blade designs.

Fig. 6 shows the same levels obtained for operating conditions OC2, i.e., for a lower wind and rotational speed. In this case, the three receivers are slightly shifted

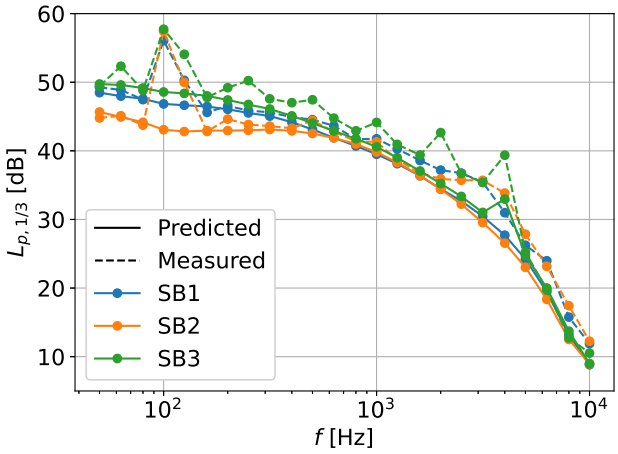

Figure 6: Comparison of the measured (dashed lines) and auralized (solid lines) 1/3 octave band levels for receivers SB1, SB2, and SB3, and operating conditions OC2.

from the upwind, crosswind and downwind directions as seen in Fig. 3. The agreement between calculated and measured levels is improved compared to higher wind conditions OC1 for receivers SB1 and SB2 with differences smaller than 2 dB over most frequencies. The measured levels for SB3 do not follow as closely the calculated levels, with differences between 2 dB and 4 dB over most frequencies. In the 100 Hz band, the difference reaches between 9 dB and 14 dB. Looking at the narrow band spectra of the recorded signals and listening to the audio signal reveals that the difference might be due to the presence of mechanical noise, as for conditions OC1, with a greater relative amplitude due to the lower levels of leading edge noise at this lower rotational speed.

4.2 Listening tests

Listening tests were performed to evaluate the ability of the proposed auralization approach to replace in-situ audio recordings for noise annoyance studies and demonstrators. As a first result, these tests were aimed at assessing the perceived realism of the auralized audio samples. A panel of 20 subjects, none of them experts in the field, with no experience in wind turbine noise and with no hearing problems, were asked to give a grade between 0 and 10 using integer values for each of the 12 audio samples. The samples are approximately 15 s long, corresponding to 4 blade rotations. They correspond to the three receivers, SB1, SB2, and SB3, for the two operating conditions OC1 and OC2, and the two sample types, recorded and auralized. The samples are presented in a random order, with the additional constraint of no more than 3 consecutive samples of the same type. The subject may repeat a given sample as desired but must move to the next sample once the note is given. The reproduction system includes a RME Babyface audio interface and a pair of Senheiser HD600 headphones. The system is calibrated with binaural dummy head and a 1000 Hz tone, assuming a flat frequency response, to ensure the reproduction of the correct sound pressure levels. The tests are carried out in a quiet room with a measured background noise level of 31 dB(A). Prior to the test, the subject reads the following instructions: “You will listen to 12 audio samples of wind turbine noise of 15 s each. Imagine yourself outside in the vicinity of an operating wind turbine. For each sample, evaluate the realism with a note on a 0 (small) to 10 (large) scale. You may listen to the sample several times. You must move to the next sample once your note is given.”.

Fig. 7a presents the realism scores, shown as box and whisker plots, considering first, all receivers and operating conditions (top two scores) and second, all receivers of the same operating conditions (lower four scores). Considering all receivers and operating conditions, results show a perceived level of realism comparable for both recorded and auralized samples. The median is 6 in both cases with an average value of 6.16 and 5.83 for the recorded and auralized samples, respectively. Now looking at the two op-

erating conditions separately, the scores of realism show similar trends. The auralized samples for the higher wind conditions, OC1, yield a slightly improved averaged score than conditions, OC2, the median value remaining at 6 for all cases. The audible presence of mechanical noise which is not included in the model does not affect the realism for non-experts listeners. The spread of the perceived realism is slightly larger for the recorded samples. A possible explanation is the presence of additional noise sources, such as mechanical noise, leading to different interpretations of the associated signal features depending on the subject. Now considering scores of realism for each receiver (Fig. 7b), the auralized samples have averaged and median values that are equal of very close to the recorded samples, Overall, it is not possible to identify a receiver or operating conditions that perform significantly better or worse than the average. Therefore, the proposed approach has the same level of realism for the three receiver positions (upwind, crosswind, and downwind) and the two sets of operating conditions.

5. CONCLUSIONS

This paper presents first validation results of a cost-efficient numerical method for wind turbine noise prediction and auralization. The method is physics-based. It includes a model of the leading- and trailing-edge noise emission, coupled with the Harmonoise far-field propagation model. In addition to averaged and instantaneous sound pressure levels, the approach allows the generation of audio signals, representative of the wind turbine noise. These auralized samples can be used in assessing noise annoyance through listening tests or describing specific noise features with psycho-acoustics indices.

For this validation study, noise spectra are calculated for three receivers' positions, approximately 150 m from the closest turbine, and two operating conditions. Five turbines are included in the simulation. The difference between the predicted and measured levels is under 4 dB in the frequency ranges where the modeled noise sources (i.e. leading- and trailing-edge noise) are dominant. Next, listening tests were performed with 20 non-expert subjects to evaluate the realism of the auralized signals. No statistical evidence suggests that the auralized signals are less realistic than the recorded signals, even when considering the operating conditions and the receivers separately.

Ongoing work is assessing the accuracy of the predicted spectra and the realism of the auralized signals for long-range propagation beyond 500 m.

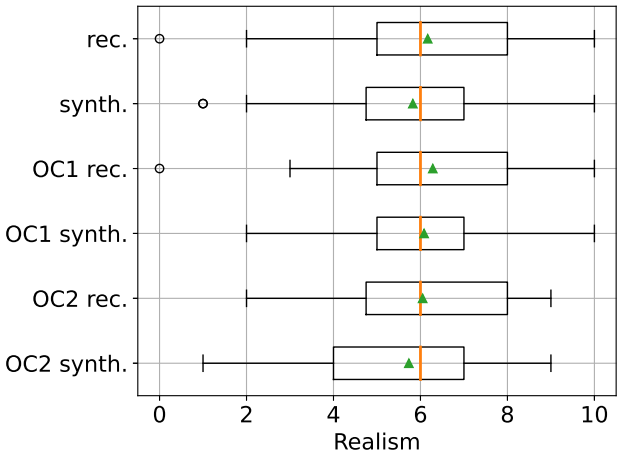

(a)

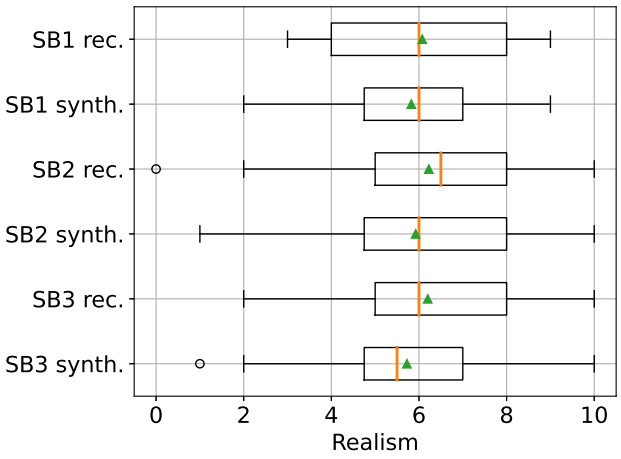

(b)

Figure 7: Perceived realism of recorded (rec) and auralized (synth) audio samples, considering (a) all receivers and operating conditions (top two scores) and conditions OC1 and OC2, separately, and (b) receivers separately. The boxplot shows the average score (green marker), the median value (orange bar), the 25 to 75% spread (black box), the statistical minimum and maximum values (black bar), and the outliers (black circles).

6. ACKNOWLEDGMENTS

This research was supported by the European Commission through the H2020-MSCA-ITN-209 project zEPHYR (grant agreement No 860101). The authors also thank UMRAE for contributing to the experimental measurement campaign used in this work.

7. REFERENCES

[1] S. A. Janssen, H. Vos, A. R. Eisses, and E. Pedersen, "A comparison between exposure-response relationships for wind turbine annoyance and annoyance due to other noise sources," *The Journal of the Acoustical Society of America*, vol. 130, no. 6, pp. 3746–3753, 2011.

[2] R. Pieren, K. Heutschi, M. Müller, M. Manyoky, and K. Eggenschwiler, "Auralization of wind turbine noise: Emission synthesis," *Acta Acustica united with Acustica*, vol. 100, no. 1, pp. 25–33, 2014.

[3] R. K. Amiet, "Acoustic radiation from an airfoil in a turbulent stream," *Journal of Sound and Vibration*, vol. 41, no. 4, pp. 407 – 420, 1975.

[4] R. K. Amiet, "Noise due to turbulent flow past a trailing edge," *Journal of Sound and Vibration*, vol. 47, no. 3, pp. 387 – 393, 1976.

[5] D. Mascarenhas, B. Cotté, and O. Doaré, "Synthesis of wind turbine trailing edge noise in free field," *JASA Express Letters*, vol. 2, p. 033601, 3 2022.

[6] B. Cotté, "Coupling of an aeroacoustic model and a parabolic equation code for long range wind turbine noise propagation," *Journal of Sound and Vibration*, vol. 422, pp. 343–357, 2018.

[7] J. Maillard and J. Jagla, "Auralization of urban traffic noise - quantitative and perceptual validation," in *Proc. of Congrès Français d'Acoustique (CFA), 22-25 April 2014, Poitiers, France*, 2014.

[8] J. Maillard and A. Kacem, "Auralization applied to the evaluation of pedestrian and bike paths in urban environments," in *Proc. of Internoise 2016, Hamburg, Germany, August 21-24*, 2016.

[9] J. Maillard, A. Kacem, N. Martin, and B. Faure, "Physically-based auralization of railway rolling noise," in *Proc. of the 23rd International Congress on Acoustics, 9-13 September, Aachen, Germany*, 2019.

[10] Y. Tian and B. Cotté, "Wind turbine noise modeling based on Amiet's theory: Effects of wind shear and atmospheric turbulence," *Acta Acustica united with Acustica*, vol. 102, no. 4, pp. 626–639, 2016.

[11] A. P. C. Bresciani, U. Boatto, S. L. Bras, P. Bonnet, and L. D. de Santana, "Influence of blade deflections on wind turbine noise directivity," *Journal of Physics: Conference Series*, vol. 2257, p. 012012, 4 2022.

[12] E. Salomons, D. Van Maercke, J. Defrance, and F. De Roo, "The Harmonoise sound propagation model," *Acta Acustica united with Acustica*, vol. 97, no. 1, pp. 62–74, 2011.

[13] D. van Maercke and J. Defrance, "Development of an analytical model for outdoor sound propagation within the harmonoise project," *Acta Acustica united with Acustica*, vol. 93, pp. 201–212, 2007.

[14] A. P. Bresciani, S. Le Bras, and L. D. de Santana, "Generalization of amiet's theory for small reduced-frequency and nearly-critical gusts," *Journal of Sound and Vibration*, vol. 524, p. 116742, 2022.

[15] A. P. C. Bresciani, J. Maillard, and L. D. de Santana, "Perceptual evaluation of wind turbine noise," in *Proc. of 16ème Congrès Français d'Acoustique*, 2022.

[16] A. P. C. Bresciani, J. Maillard, and L. D. de Santana, "Physics-based scintillations for outdoor sound auralization," 2023. Submitted to *The Journal of the Acoustical Society of America*.

[17] A. P. C. Bresciani, J. Maillard, S. Le Bras, and L. D. de Santana, "Wind turbine noise synthesis from numerical simulations," 2023. Accepted for publication in 29^{th} AIAA/CEAS Aeroacoustics Conference.

[18] M. Churchfield, "A method for designing generic wind turbine models representative of real turbines and generic Siemens SWT-2.3-93 and Vestas V80 specifications," *National Renewable Energy Laboratory, Golden, Colorado*, 2013.

[19] J. Christophe, S. Buckingham, C. Schram, and S. Oerlemans, "zEPHYR - large on shore wind turbine benchmark." Data set, Mar. 2022.

[20] "Weather spark." `https://fr.weatherspark.com`. Accessed: 2023-04-28.